Research Square

Preprints are preliminary reports that have not undergone peer review.
They should not be considered conclusive, used to inform clinical practice,
or referenced by the media as validated information.

Regional reorganization of long-range climate persistence under global warming

Jouni Takalo

jojuta@gmail.com

Research Article

Keywords: climate persistence, detrended fluctuation analysis, long-range correlations, climate dynamics

Posted Date: June 1st, 2026

DOI: https://doi.org/10.21203/rs.3.rs-9768367/v1

License: This work is licensed under a Creative Commons Attribution 4.0 International License.
Read Full License

Additional Declarations: No competing interests reported.

Regional reorganization of long-range climate persistence under global warming

Jouni Takalo

Docent, University of Jyväskylä, Oulu, 90910, Finland.

Contributing authors: jojuta@gmail.com;

Abstract

Climate change is expected to modify not only mean climatic conditions but also the temporal persistence and memory structure of climate variability. However, the long-term evolution of climatic persistence under global warming remains poorly understood, particularly for regional hydroclimatic systems and precipitation variability.

Here, we investigate the temporal evolution of long-range persistence in monthly temperature and precipitation anomalies during 1901–2023 using detrended fluctuation analysis (DFA) with sliding 30-year windows. The analysis is based primarily on the CRU TS observational dataset and is supplemented by ERA5 reanalysis and GPCC precipitation observations for robustness assessment. Spatial persistence changes are examined globally and within major climatic regimes including the Arctic, Northern Hemisphere midlatitudes, the tropics, Monsoon Asia, Europe, and the Amazon basin.

The results reveal a pronounced regional reorganization of climate persistence under global warming. Temperature persistence strengthens substantially across Northern Hemisphere midlatitudes, while several tropical and Arctic regions exhibit weakening long-range memory. Tropical temperatures maintain exceptionally strong persistence throughout the observational period ($\boldsymbol{\alpha \approx 1}$), consistent with dominant oceanic thermal memory and large-scale coupled variability. In contrast, precipitation generally remains substantially less persistent and closer to random behavior ($\boldsymbol{\alpha \approx 0.5}$–$\boldsymbol{0.7}$), reflecting the intermittent and episodic nature of hydrological processes. Monsoon Asia displays particularly weak and highly variable precipitation persistence despite relatively persistent temperature variability, suggesting strong seasonal resetting of the monsoon system. Comparisons between CRU, ERA5, and GPCC further demonstrate that the major multi-decadal persistence transitions are robust across independent datasets.

These findings suggest that climate change affects not only mean states and variance characteristics but also the intrinsic temporal organization of the climate

system itself. The observed persistence transitions indicate that ongoing warming is associated with large-scale dynamical restructuring of climate memory, hydrological intermittency, and regional climate stability.

Keywords: climate persistence, detrended fluctuation analysis, long-range correlations, climate dynamics

1 Introduction

Climate variability exhibits complex temporal correlations over a wide range of spatial and temporal scales. One of the most intriguing properties of climatic systems is the existence of long-range persistence (LRP), where fluctuations remain statistically correlated over long time intervals [1–3]. Such persistence has been observed in atmospheric temperature, ocean temperatures, hydrological records, and precipitation variability [4–9].

Long-range persistence is commonly characterized by the scaling exponent α, which describes how temporal correlations decay with increasing timescale. For uncorrelated random variability, $\alpha = 0.5$, while values $\alpha > 0.5$ indicate persistent behavior and long-term memory. In climatic systems, persistence reflects the combined effects of oceanic heat storage, atmospheric circulation, land–ocean coupling, and large-scale circulation modes [5, 6, 8].

Detrended fluctuation analysis (DFA) has become one of the standard methods for quantifying long-range persistence in nonstationary climatic time series [10–12]. Unlike classical autocorrelation or rescaled-range methods, DFA is relatively robust against trends and low-frequency nonstationarities [13, 14], making it particularly suitable for climate applications where secular warming trends are present [6, 9]. The method has been widely applied in atmospheric and hydrological analyses [4, 7, 15, 16].

Previous studies have shown that monthly surface air temperatures typically exhibit persistent scaling behavior with DFA exponents around $\alpha \approx 0.6$–0.9 [4, 6, 7, 17]. Persistence tends to be stronger over oceans than over land because of the large thermal inertia of the ocean mixed layer [5, 6, 8]. This behavior has been linked to long-range dependence and scale-invariant climate dynamics arising from multi-timescale ocean–atmosphere coupling and energy balance processes [18]. Several studies have furthermore demonstrated systematic geographical dependence in persistence, including latitude-dependent scaling behavior [9, 19–21]. Recent work has also reported increasing persistence of warm and wet winter conditions in northwestern Europe associated with large-scale circulation variability and persistent positive NAO phases [22].

In contrast, precipitation generally exhibits substantially weaker persistence and often remains close to random behavior ($\alpha \approx 0.5$), reflecting the intermittent and highly nonlinear nature of hydrological processes [15, 16, 23–25]. However, strong regional differences exist, and tropical as well as monsoon-dominated regions can exhibit pronounced long-range persistence in precipitation variability [26].

The interpretation of persistence in precipitation remains particularly challenging. Some studies have suggested weak but significant long-range persistence in rainfall

variability [15, 24, 27], whereas others emphasize strong scale dependence and regional heterogeneity [16, 25, 26]. Hydrological persistence is likely influenced by the combined effects of convective intermittency, large-scale circulation variability, land–atmosphere coupling, and monsoonal dynamics. Recent studies further suggest that persistence changes in precipitation may be dynamically linked to shifts in atmospheric circulation regimes such as the North Atlantic Oscillation [22].

In an earlier study, we investigated persistence of temperature and precipitation anomalies from local to hemispheric and global scales using DFA [28]. We showed that the scaling exponent of temperature increases systematically when moving from local observations toward larger spatial averages. Furthermore, we demonstrated that the persistence of temperature anomalies decreases poleward in both hemispheres, with equatorial regions exhibiting the strongest long-range correlations. Precipitation persistence was found to be weaker and more dependent on regional climate regimes than temperature persistence.

Despite the extensive literature on climatic persistence, much less attention has been paid to the temporal evolution of persistence itself. Most previous studies have estimated a single scaling exponent over the entire observational interval, implicitly assuming stationarity of the persistence structure. However, ongoing anthropogenic climate change may alter the memory properties of the climate system through changes in Arctic amplification, ocean-atmosphere coupling, monsoon dynamics, hydrological intensification, and large-scale circulation variability [29–31].

Recent studies have also suggested that climate warming may modify not only mean states but also the magnitude, persistence, and intermittency of climate variability [29, 30]. Such changes may be particularly important in high-latitude regions undergoing rapid Arctic amplification, as well as in hydrological systems where intensified moisture transport may enhance episodic precipitation extremes.

The purpose of the present study is therefore to investigate how climatic persistence has evolved during the twentieth and early twenty-first centuries. Using sliding-window detrended fluctuation analysis, we analyze temporal changes in the scaling exponent of regional temperature and precipitation anomalies. The analysis is performed for multiple climatic regions using independent datasets including CRU TS [32], ERA5 reanalysis, and GPCC precipitation observations.

Particular attention is given to differences between temperature and precipitation persistence, regional contrasts between tropical and high-latitude climates, and possible indications of changing large-scale climate dynamics. We show that temperature persistence generally weakens in several high-latitude regions during recent decades, while precipitation persistence exhibits stronger regional dependence and substantially weaker long-range memory.

2 Data and Methods

2.1 Datasets

To investigate the temporal evolution of long-range climate persistence, three independent gridded climate datasets were analyzed.

- **CRU TS v4.08** monthly temperature and precipitation data covering the period 1901–2023 were used as the primary historical dataset. The CRU dataset provides land-based gridded observations at $0.5^\circ \times 0.5^\circ$ spatial resolution.
- **ERA5 reanalysis** monthly mean near-surface air temperature (2 m temperature) and total precipitation were used for modern-period validation. ERA5 provides dynamically consistent atmospheric reanalysis fields at high spatial resolution ($0.25^\circ \times 0.25^\circ$). The analysis primarily focused on the period after 1950, when observational constraints become substantially more reliable.
- **GPCC Full Data Monthly v2022** precipitation data covering 1891–2020 were used as an independent gauge-based validation dataset for hydrological persistence. GPCC is based on quality-controlled rain gauge observations and is widely used in large-scale hydrological studies.

All analyses were performed using monthly mean data.

2.2 Regional Averaging

Regional climate indices were constructed using area-weighted spatial averages over selected latitude–longitude domains. Grid-cell contributions were weighted by the cosine of latitude in order to account for the decreasing physical area of grid cells toward the poles.

The investigated regions included:

- Tropics (20°S–20°N),
- Northern Hemisphere mid-latitudes (30°N–60°N),
- Arctic/sub-Arctic regions,
- Europe,
- Monsoon Asia,
- Amazon basin.

2.3 Anomaly Construction

Monthly anomalies were calculated by removing the climatological seasonal cycle separately for each calendar month:

$$x'(t) = x(t) - \overline{x}_m, \tag{1}$$

where $\overline{x}_m$ denotes the long-term mean value for calendar month m (January, February, ..., December). This procedure removes the dominant annual cycle and allows DFA to characterize long-range temporal correlations in the anomaly variability itself rather than the deterministic seasonal signal.

Because precipitation exhibits highly skewed distributions and strong intermittency, precipitation fields were variance-stabilized prior to anomaly construction using the transformation

$$P'(t) = \log_{10}(P(t) + 1), \tag{2}$$

where $P(t)$ denotes monthly precipitation. The logarithmic transformation reduces the influence of extreme rainfall events and improves the stability of the DFA scaling estimates.

2.4 Detrended Fluctuation Analysis (DFA)

Long-range temporal persistence was quantified using detrended fluctuation analysis (DFA), a widely used method for detecting scaling behavior in nonstationary time series [33, 34]. DFA is particularly suitable for climatic applications because it provides robust scaling estimates in the presence of trends and low-frequency variability.

For an anomaly series x_i, the integrated profile was first constructed as

$$Y(k) = \sum_{i=1}^{k} (x_i - \bar{x}) \,, \tag{3}$$

where $\bar{x}$ is the temporal mean of the series.

The integrated profile was then divided into segments of length L. Within each segment, local polynomial trends were removed using first-order detrending. The root-mean-square fluctuation function was subsequently computed as

$$F(L) = \sqrt{\frac{1}{N} \sum_{k=1}^{N} [Y(k) - Y_{\mathrm{fit}}(k)]^2}, \tag{4}$$

where $Y_{\mathrm{fit}}(k)$ denotes the local polynomial trend.

If the fluctuations obey scale-invariant long-range correlations, the fluctuation function follows a power-law relationship,

$$F(L) \sim L^{\alpha}, \tag{5}$$

where α is the DFA scaling exponent.

The scaling exponent was estimated from linear regression in log–log space over time scales ranging from 12 to 96 months.

2.5 Interpretation of the Scaling Exponent

The DFA scaling exponent α characterizes the temporal memory structure of climate variability:

- $\alpha = 0.5$: uncorrelated white-noise behavior,
- $0.5 < \alpha < 1$: persistent long-range correlations,
- $\alpha < 0.5$: anti-persistent behavior,
- $\alpha \approx 1$: very strong persistence and slow-decaying memory.

In the present study, increasing α values indicate strengthening temporal persistence, whereas decreasing α values suggest enhanced intermittency, reduced memory, or increasingly episodic variability.

2.6 Sliding-Window Persistence Analysis

To investigate the temporal evolution of persistence, DFA was applied within moving 30-year windows advanced in 1-year increments. This produced time-dependent estimates of the scaling exponent $\alpha(t)$ for both temperature and precipitation.

To suppress high-frequency estimation noise and emphasize multi-decadal behavior, the resulting sliding-window α series were additionally smoothed using an 11-year moving average for visualization purposes.

2.7 Cross-Dataset Validation

The robustness of the persistence patterns was evaluated by comparing corresponding regional results across independent datasets (CRU, ERA5, and GPCC). Consistent persistence behavior across datasets was interpreted as evidence that the observed scaling structures are unlikely to arise solely from dataset-specific interpolation methods or observational artifacts.

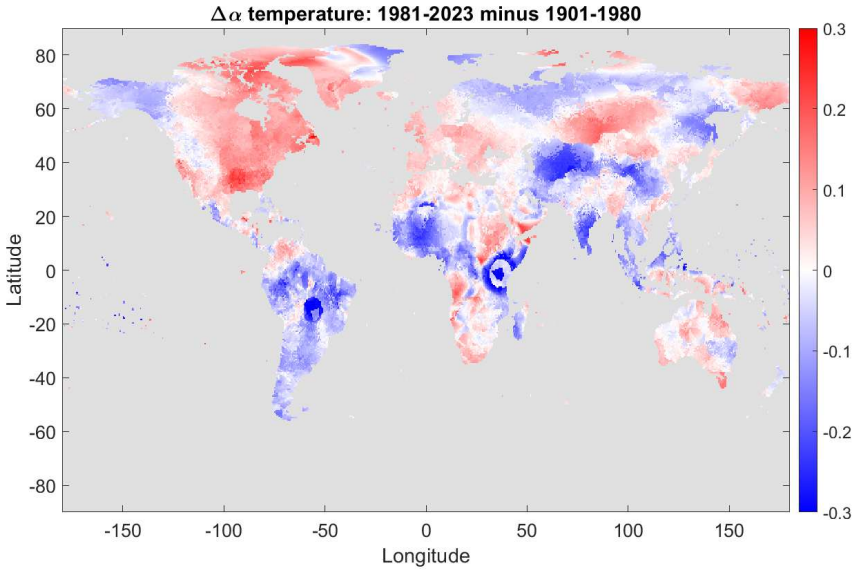


Fig. 1 Spatial distribution of changes in temperature persistence between the periods 1901–1980 and 1981–2023, quantified using the difference in DFA scaling exponent $\Delta\alpha$. Positive values (red) indicate strengthening long-range persistence, whereas negative values (blue) denote weakening persistence. Persistence changes are spatially heterogeneous and organized into large-scale climatic regimes. Enhanced persistence is particularly evident over Northern Hemisphere mid-latitudes, while several tropical land regions, including the Amazon and Congo basins, exhibit slightly reduced persistence.

3 Results

3.1 Regional Observations and Physical Mechanisms

3.1.1 Amazon & Tropics: Extreme Thermal Persistence

Observations: Both the Amazon and the broader tropical band exhibit persistently high temperature scaling exponents throughout the observational period, with α

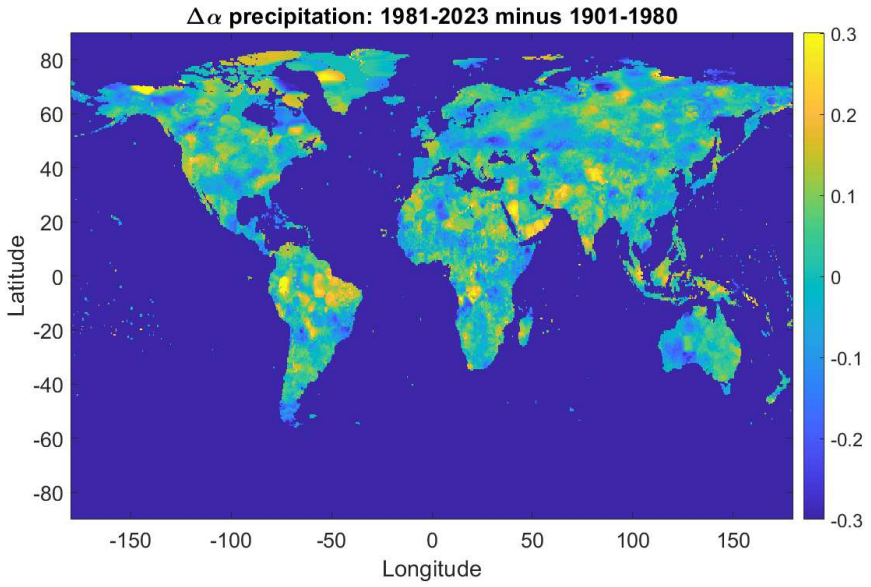


Fig. 2 Spatial distribution of changes in precipitation persistence ($\Delta\alpha$) between 1901–1980 and 1981–2023 derived from monthly CRU TS precipitation anomalies using detrended fluctuation analysis (DFA). Compared with temperature persistence, precipitation persistence exhibits a substantially more fragmented and spatially heterogeneous structure, with localized regions of both increasing and decreasing long-range memory. The patchy organization reflects the intermittent and regionally complex nature of hydrological variability, including convective processes, monsoonal dynamics, and localized land–atmosphere interactions.

values remaining close to or above 1.0 after the mid-20th century. However, the spatial $\Delta\alpha$ analysis indicates that several tropical land regions, including parts of the Amazon and Congo basins, experienced a moderate reduction in persistence during the late-period climate relative to the mid-twentieth century.

Physical Drivers:

- **Sea Surface Temperature (SST) Dominance:** The tropical continental climate is tightly coupled to the surrounding oceans (e.g., ENSO nodes and Atlantic multidecadal modes). As oceans warm, their thermal inertia increases, releasing energy into the atmosphere more uniformly and extending the memory of atmospheric anomalies.
- **Biosphere-Atmosphere Feedbacks (Amazon):** The intense evapotranspiration of the Amazon rainforest sustains a closed-loop hydrological cycle. Severe warming or deforestation degrades this recycling capacity, trapping the regional subsystem into prolonged "dry/hot" states, which manifests as an elevated α.

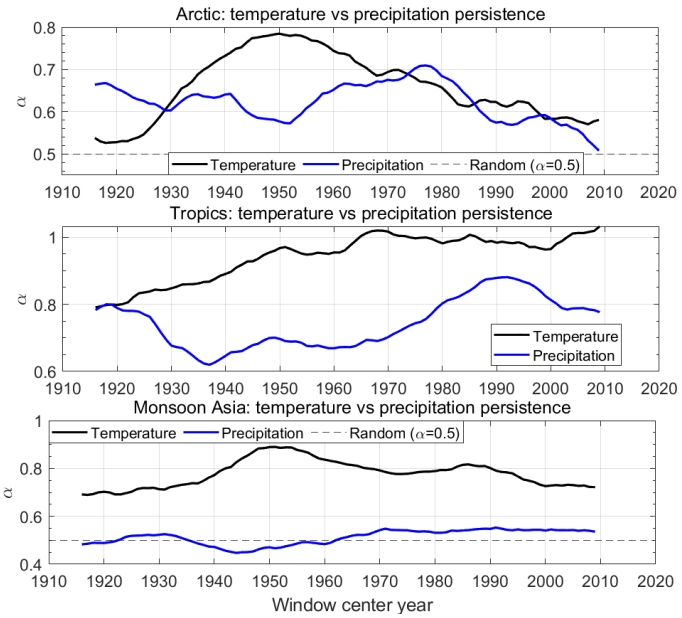


Fig. 3 Comparison of temperature and precipitation persistence evolution for three major climatic regimes: the Arctic (top), Tropics (middle), and Monsoon Asia (bottom). Persistence is quantified using the DFA scaling exponent α computed from monthly anomaly series. Black curves denote temperature persistence, while blue curves represent precipitation persistence. The dashed horizontal line marks the random non-persistent limit ($\alpha = 0.5$). Temperature anomalies exhibit systematically stronger long-range persistence than precipitation anomalies in all regions. The contrast is particularly pronounced in Monsoon Asia, where precipitation remains close to the random threshold despite highly persistent temperature variability, reflecting strong seasonal resetting of the monsoon system. Tropical regions maintain exceptionally high persistence in both variables, consistent with dominant oceanic memory and large-scale coupled climate variability. In contrast, Arctic persistence weakens in recent decades for both temperature and precipitation, suggesting increasing dynamical instability in the rapidly changing Arctic climate system.

3.1.2 The Arctic: Decadal Persistence Decline

Observations: The Arctic features a dramatic, large-scale wave-like modulation. Temperature persistence peaks significantly ($\alpha \approx 0.78$) during the 1940s–1950s before undergoing a sharp, steady decline toward the present day, reaching approximately $\alpha \approx 0.57$. Precipitation follows a similar trajectory with a slight phase lag, collapsing recently toward pure randomness ($\alpha \approx 0.5$).

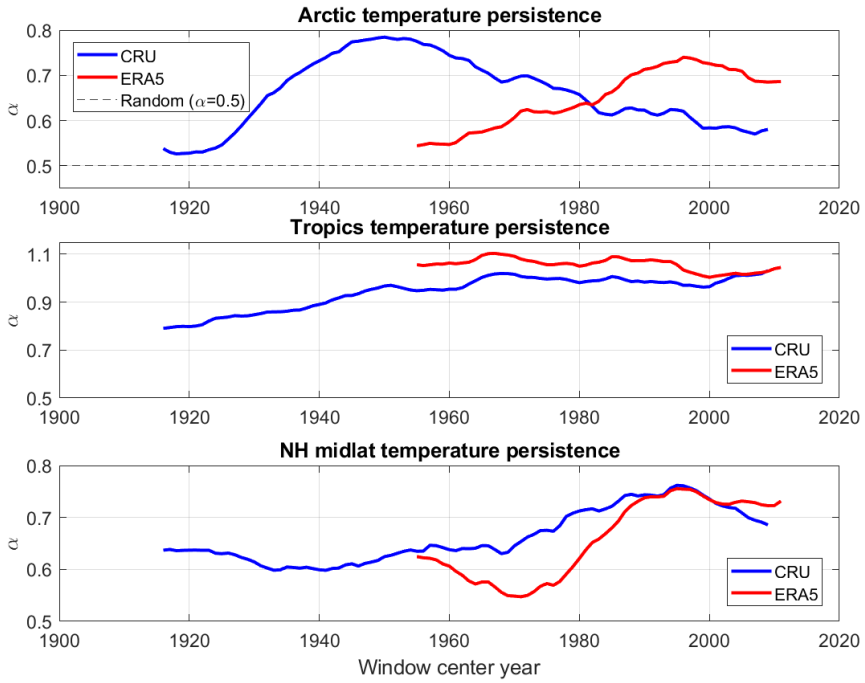


Fig. 4 Temporal evolution of regional temperature persistence quantified by the DFA scaling exponent α for three major climatic regimes: the Arctic (top), Tropics (middle), and Northern Hemisphere mid-latitudes (bottom). Blue curves denote CRU TS observations, while red curves represent ERA5 reanalysis results. The dashed horizontal line indicates the random non-persistent limit ($\alpha = 0.5$). Despite differences in observational coverage and assimilation methodology, both datasets reproduce the same broad persistence regimes. Tropical temperatures maintain exceptionally strong long-range persistence throughout the observational period, whereas Northern Hemisphere mid-latitudes exhibit increasing persistence during the late twentieth century. Arctic persistence weakens during recent decades, although the timing differs between CRU and ERA5.

Physical Drivers:

- **Arctic Amplification and Sea Ice Loss:** Accelerated sea ice decline in recent decades has exposed vast expanses of open ocean. Stripped of its insulating ice cover, the lower atmosphere responds rapidly and directly to diurnal and seasonal radiative forcing. This increases the influence of short-timescale variability and episodic atmospheric processes, shifting the Arctic climate system toward weaker long-range persistence and more noise-like behavior.
- **Atlantic Multidecadal Oscillation (AMO):** The prominent mid-century peak strongly correlates with the warm phase of the AMO, which enhanced poleward heat transport and temporarily stabilized large-scale Arctic atmospheric persistence.

3.1.3 Northern Hemisphere Mid-Latitudes: Divergent Coupled Trends

Observations: This region displays highly anomalous behavior where temperature and precipitation trends diverge completely. Northern Hemisphere midlatitude precipitation exhibits pronounced multi-decadal variability in persistence. Persistence weakened from the early twentieth century toward near-random behavior during the 1970s and early 1980s, after which a strong recovery occurred, with α increasing again during recent decades. Simultaneously, temperature persistence grew steadily from $\alpha \approx 0.6$ to $\alpha \approx 0.75$.

Physical Drivers:

- **Acceleration of the Hydrological Cycle (Precipitation):** In accordance with the Clausius-Clapeyron relation, a warmer mid-latitude atmosphere holds more moisture. This has shifted precipitation regimes from steady frontal systems toward highly episodic, convective, and localized storm events. This mechanism may contribute to the observed reduction in precipitation persistence during mid-twentieth century.
- **Jet Stream Meandering and Wave Resonance (Temperature):** Enhanced Arctic warming reduces the equator-to-pole thermal gradient. A reduced equator-to-pole temperature gradient may promote more persistent and meandering jet stream configurations. Such circulation regimes can prolong regional thermal anomalies and may therefore contribute to increasing temperature persistence (α).

3.1.4 Europe: The Double-Peak Profile

Observations: Temperature persistence in Europe exhibits a distinct bimodal structure, with two prominent maxima ($\alpha \approx 0.78$) centered in the 1940s and 1980s, separated by a sharp decline in the 1960s. Conversely, precipitation persistence shows a long-term downward trend post-1930, hovering near the white noise threshold ($\alpha \approx 0.5$) in the modern era.

Physical Drivers:

- **North Atlantic Oscillation (NAO) and Jet Stream Dynamics:** European weather is heavily dictated by the jet stream. The dual temperature peaks coincide with epochs characterized by high atmospheric blocking frequency, which locks synoptic weather patterns in place for extended periods.
- **Anthropogenic Aerosols (1950–1970):** Heavy industrial sulfur emissions in Europe peaked during the 1960s, inducing regional "global dimming".The mid-century decline may also have been influenced by strong anthropogenic aerosol forcing during the European dimming period. Post-regulation clean-up in the 1980s allowed natural persistence to rebound.

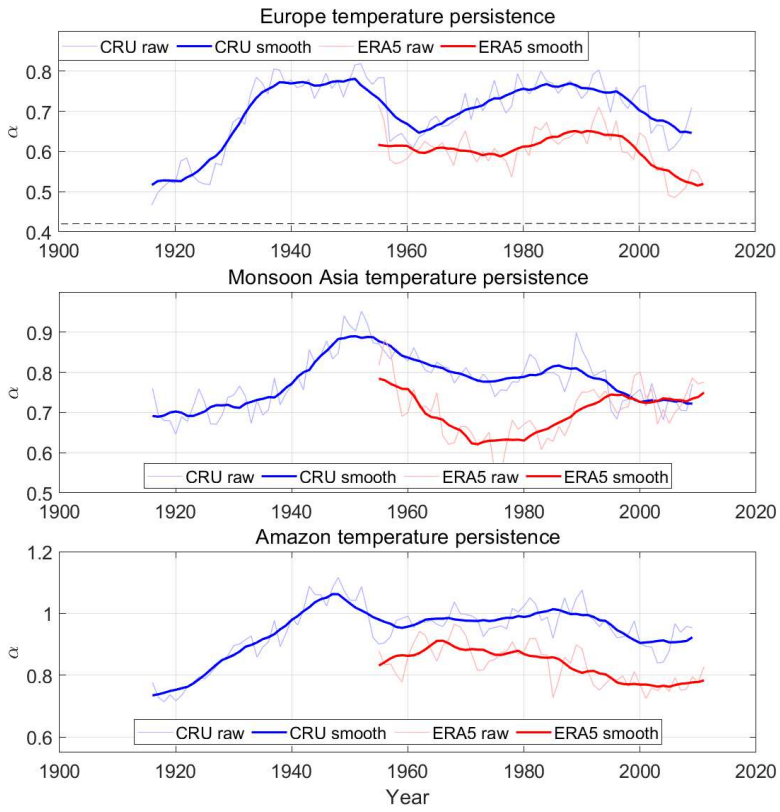


Fig. 5 Additional CRU–ERA5 comparisons of regional temperature persistence for Europe (top), Monsoon Asia (middle), and the Amazon basin (bottom). Despite differences in observational methodology and temporal coverage, the major multi-decadal persistence transitions are consistently reproduced in both datasets. The agreement is particularly strong for the timing of the mid-century persistence maxima and subsequent late-century weakening trends.

3.1.5 Monsoon Asia: Seasonal Constraint and Weak Hydrological Memory

Observations: Temperature persistence in the monsoon region reaches elevated values during the mid-20th century before gradually stabilizing around $\alpha \approx 0.7$. In contrast, precipitation persistence remains substantially weaker and exhibits stronger temporal variability. In some periods, the precipitation scaling exponent approaches or briefly falls below the random threshold ($\alpha \approx 0.5$), indicating weak long-range persistence and possible anti-persistent tendencies. Compared with other regions, the precipitation behavior in Monsoon Asia also appears more dataset-sensitive.

Possible Physical Mechanisms:

- **Strong Seasonal Forcing:** The Asian monsoon is dominated by a highly regular seasonal land–ocean thermal contrast. This externally forced annual cycle may limit

the development of very long hydrological memory, because precipitation anomalies are repeatedly reset by the onset of subsequent monsoon seasons.

- **Intermittent Convective Dynamics:** Monsoonal precipitation is strongly influenced by episodic convection, intraseasonal oscillations, and regional circulation variability. Such processes may produce relatively rapid alternation between wet and dry conditions, thereby suppressing long-range persistence in precipitation compared with temperature.
- **Regional Complexity and Dataset Sensitivity:** The monsoon domain combines diverse climatic subregions, including the Indian monsoon, Southeast Asian convection zones, and western Pacific influences. The differing behavior between datasets suggests that the persistence structure may vary considerably within the broader monsoon system itself.

4 Discussion

The present results demonstrate that long-range climate persistence is not stationary under global warming but undergoes substantial regional reorganization across both temperature and precipitation fields. The observed changes are spatially coherent in some regions yet highly fragmented in others, indicating that climate change alters not only mean climatic conditions but also the internal temporal organization and stability properties of regional climate subsystems.

4.1 Low-Latitude Thermal Memory and High-Latitude Dynamical Variability

The tropical regions and the Amazon basin exhibit exceptionally strong and temporally stable temperature persistence throughout the observational period, with scaling exponents approaching $\alpha \approx 1$. This behavior suggests very slowly decaying climatic memory associated with strong oceanic coupling, ENSO-scale variability, and the large thermal inertia of tropical oceans. As anthropogenic warming increases sea surface temperatures, the large heat capacity of the tropical oceans may further enhance low-frequency thermal memory in the overlying atmosphere.

In the Amazon basin, persistent land–atmosphere feedbacks may additionally contribute to prolonged climatic anomalies. Moisture recycling through intense evapotranspiration acts as an internal memory mechanism linking soil moisture, vegetation, and atmospheric humidity. Changes in rainforest functioning and regional hydrological stress may therefore influence the temporal persistence structure of the Amazon climate system itself. The weaker and more variable precipitation persistence observed in the Amazon further suggests increasing hydrological intermittency despite highly persistent temperature variability.

In contrast, the Arctic exhibits a markedly different persistence evolution. Both temperature and precipitation persistence weaken substantially during recent decades, particularly after the late twentieth century. Although the aggregated Arctic persistence series exhibits a pronounced decline during recent decades, the spatial persistence maps reveal substantial regional heterogeneity within the Arctic system itself. In particular, several northern continental regions of Canada and Greenland display locally

enhanced persistence, whereas the strongest reductions occur primarily over sea-ice-dominated Arctic Ocean sectors. This contrast suggests that terrestrial and marine Arctic subsystems may respond differently to ongoing warming and sea-ice loss. The prominent mid-century persistence maximum followed by declining α values may be related to Arctic amplification and the rapid reduction of sea-ice cover. In the earlier climate state, extensive sea ice likely acted as a low-pass filter, insulating the atmosphere from rapid ocean-atmosphere heat exchange. As sea ice declines, the lower atmosphere becomes increasingly exposed to short-timescale radiative forcing, open-water heat fluxes, and episodic circulation variability. The resulting Arctic climate regime therefore appears more dynamically variable and less strongly persistent than during the mid-twentieth century. The temporal differences between CRU and ERA5 during the early Arctic period likely reflect observational limitations and sparse station coverage, although both datasets reproduce the overall long-term decline in persistence.

4.2 Atmospheric Circulation, Blocking, and Hydrological Intermittency

The Northern Hemisphere midlatitudes display a particularly interesting divergence between temperature and precipitation persistence. Temperature persistence increases steadily during the late twentieth century, whereas precipitation persistence decreases toward near-random behavior. This contrast suggests that warming may simultaneously stabilize large-scale thermal anomaly patterns while accelerating the intermittency of the hydrological cycle.

One possible explanation involves enhanced Rossby-wave amplification and persistent atmospheric blocking associated with Arctic amplification and reduced equator-to-pole temperature gradients. Slower and more meandering jet stream configurations may prolong regional temperature anomalies and thereby increase long-range thermal persistence. At the same time, according to the Clausius–Clapeyron relation, a warmer atmosphere can sustain substantially larger moisture content, favoring increasingly episodic and convectively dominated precipitation events. Such structural changes in precipitation regimes may disrupt long-range rainfall correlations and shift precipitation variability closer to white-noise behavior.

European persistence variability further emphasizes the importance of large-scale atmospheric circulation. The bimodal structure in European temperature persistence coincides qualitatively with periods of enhanced blocking frequency and North Atlantic Oscillation variability. The pronounced mid-century persistence reduction may also have been influenced by strong anthropogenic aerosol forcing during the European dimming period, which likely modified regional radiative balances and land–atmosphere coupling. Following air-quality improvements during the late twentieth century, persistence increased again toward higher values.

Monsoon Asia represents an intermediate hydroclimatic regime characterized by relatively persistent temperature variability but substantially weaker and more variable precipitation persistence. The monsoon system is strongly controlled by seasonal land–ocean thermal contrasts, which repeatedly reset hydrological anomalies during each monsoon cycle. This seasonal anchoring may limit the emergence of very

strong long-range precipitation persistence even under substantial climatic warming. In addition, monsoonal precipitation is strongly influenced by episodic convection, intraseasonal variability, and regional circulation complexity, all of which likely contribute to the highly variable and dataset-sensitive precipitation persistence observed in this region.

4.3 Robustness, Limitations, and Implications

An important outcome of the study is the high degree of structural consistency observed across independent datasets. Despite differences in observational coverage, spatial resolution, interpolation methodology, and data assimilation schemes, CRU, ERA5, and GPCC reproduce remarkably similar large-scale persistence regimes and multi-decadal transitions. This agreement strongly suggests that the observed persistence changes are physically meaningful and unlikely to arise solely from dataset-specific artifacts.

The robustness of the precipitation persistence results was additionally evaluated using the independent GPCC gauge-based precipitation dataset. The major large-scale precipitation persistence structures and temporal transitions were broadly reproduced, particularly within tropical and midlatitude regions. Larger discrepancies occurred primarily in monsoon-dominated regions where precipitation variability is strongly affected by localized convective processes and observational heterogeneity.

Several limitations nevertheless remain. Sliding-window DFA estimates are sensitive to window length, detrending order, and low-frequency variability. Precipitation persistence is particularly challenging because of strong intermittency, skewed distributions, and substantial regional heterogeneity. Furthermore, the present analysis focuses on monthly variability and therefore does not fully resolve persistence changes on synoptic or centennial timescales.

Overall, the results suggest that climate change influences not only mean states and variance characteristics but also the intrinsic temporal memory structure of the climate system itself. Persistence diagnostics may therefore provide an additional dynamical perspective for understanding evolving climate stability, hydrological variability, and large-scale circulation changes under continued global warming.

5 Conclusions

This study demonstrates that the persistence structure of the climate system has undergone substantial regional changes during the twentieth and early twenty-first centuries. The observed changes are spatially heterogeneous and differ fundamentally between temperature and precipitation.

Temperature persistence exhibits strong long-range memory over tropical and ocean-influenced regions, whereas precipitation generally remains closer to random or weakly persistent behavior. Nevertheless, several regions display clear multi-decadal transitions in persistence, indicating that climate change affects not only mean climatic conditions but also the temporal organization of climate variability itself.

The strongest persistence increases are observed over Northern Hemisphere midlatitudes, while parts of the Arctic and several tropical land regions show weakening

persistence. Monsoon Asia represents a particularly stable hydrological persistence regime despite pronounced changes in temperature persistence. Comparisons between CRU, ERA5, and GPCC datasets further indicate that the major large-scale persistence transitions are robust across independent observational products.

Overall, the results suggest that persistence provides an additional dynamical dimension for understanding climate change beyond traditional analyses of means and variances. Long-range memory diagnostics may therefore offer useful insight into evolving climate stability, hydrological variability, and the future organization of regional climate regimes.

Acknowledgments

The author acknowledges the Climatic Research Unit (CRU), the European Centre for Medium-Range Weather Forecasts (ECMWF), and the Global Precipitation Climatology Centre (GPCC) for providing the observational and reanalysis datasets used in this study. ERA5 data were obtained from the Copernicus Climate Change Service (C3S). GPCC precipitation data were provided by the Deutscher Wetterdienst (DWD).

References

[1] Hurst, H.E.: Long-term storage capacity of reservoirs. Transactions of the American Society of Civil Engineers **116**, 770–799 (1951) https://doi.org/10.1061/TACEAT.0006518

[2] Taqqu, M.S., Teverovsky, V., Willinger, W.: Estimators for long-range dependence: An empirical study. Fractals **3**(4), 785–798 (1995) https://doi.org/10.1142/S0218348X95000692

[3] Graves, T., Gramacy, R., Watkins, N., Franzke, C.: A brief history of long memory: Hurst, mandelbrot and the road to arfima, 1951–1980. Entropy **19**(9), 437 (2017) https://doi.org/10.3390/e19090437

[4] Koscielny-Bunde, E., Bunde, A., Havlin, S., Roman, H.E., Goldreich, Y., Schellnhuber, H.-J.: Indication of a universal persistence law governing atmospheric variability. Physical Review Letters **81**(3), 729–732 (1998) https://doi.org/10.1103/PhysRevLett.81.729

[5] Bunde, A., Havlin, S.: Power-law persistence in the atmosphere and in the oceans. Physica A **314**(1–4), 15–24 (2002) https://doi.org/10.1016/S0378-4371(02)01050-6

[6] Fraedrich, K., Blender, R.: Scaling of atmosphere and ocean temperature correlations in observations and climate models. Physical Review Letters **90**(10), 108501 (2003) https://doi.org/10.1103/PhysRevLett.90.108501

[7] Eichner, J.F., Koscielny-Bunde, E., Bunde, A., Havlin, S., Schellnhuber, H.J.: Power-law persistence and trends in the atmosphere: A detailed study of long temperature records. Physical Review E **68**(4), 046133 (2003) https://doi.org/10.1103/PhysRevE.68.046133

[8] Monetti, R.A., Havlin, S., Bunde, A.: Long-term persistence in the sea surface temperature fluctuations. Physica A **320**, 581–589 (2003) https://doi.org/10.1016/S0378-4371(02)01662-X

[9] Blesić, S., Zanchettin, D., Rubino, A.: Heterogeneity of scaling of the observed global temperature data. Journal of Climate **32**(2), 349–367 (2019) https://doi.org/10.1175/JCLI-D-18-0211.1

[10] Kantelhardt, J.W., Koscielny-Bunde, E., Rego, H.H.A., Havlin, S., Bunde, A.: Detecting long-range correlations with detrended fluctuation analysis. Physica A **295**(3–4), 441–454 (2001) https://doi.org/10.1016/S0378-4371(01)00144-3

[11] Kantelhardt, J.W., Zschiegner, S.A., Koscielny-Bunde, E., Havlin, S., Bunde, A., Stanley, H.E.: Multifractal detrended fluctuation analysis of nonstationary time series. Physica A **316**(1–4), 87–114 (2002) https://doi.org/10.1016/S0378-4371(02)01383-3

[12] Talkner, P., Weber, R.O.: Power spectrum and detrended fluctuation analysis: Application to daily temperatures. Physical Review E **62**(1), 150–160 (2000) https://doi.org/10.1103/PhysRevE.62.150

[13] Weron, R.: Estimating long-range dependence: finite sample properties and confidence intervals. Physica A **312**(1–2), 285–299 (2002) https://doi.org/10.1016/S0378-4371(02)00961-5

[14] Grech, D., Mazur, Z.: On the scaling ranges of detrended fluctuation analysis for long-term memory correlated short series of data. Physica A **392**(10), 2384–2397 (2013) https://doi.org/10.1016/j.physa.2013.01.049

[15] Kantelhardt, J.W., Koscielny-Bunde, E., Rybski, D., Braun, P., Havlin, S., Bunde, A.: Long-term persistence and multifractality of precipitation and river runoff records. Journal of Geophysical Research **111**(D1), 01106 (2006) https://doi.org/10.1029/2005JD005881

[16] Markonis, Y., Koutsoyiannis, D.: Scale-dependence of persistence in precipitation records. Nature Climate Change **6**(4), 399–401 (2016) https://doi.org/10.1038/nclimate2894

[17] Bunde, A., Eichner, J.F., Havlin, S., Kantelhardt, J.W.: Long-term memory: A natural mechanism for the clustering of extreme events and anomalous residual times in climate records. Physical Review Letters **94**(4), 048701 (2005) https://doi.org/10.1103/PhysRevLett.94.048701

[18] Fredriksen, H.-B., Rypdal, K.: Long-range persistence in global surface temperatures explained by linear multi-box energy balance models. Journal of Climate **30**(18), 7157–7168 (2017) https://doi.org/10.1175/JCLI-D-16-0877.1

[19] Király, A., Jánosi, I.M.: Detrended fluctuation analysis of daily temperature records: Geographic dependence over australia. Meteorology and Atmospheric Physics **88**, 119–128 (2005) https://doi.org/10.1007/s00703-004-0078-7

[20] Király, A., Bartos, I., Jánosi, I.M.: Correlation properties of daily temperature anomalies over land. Tellus A **58**(5), 593–600 (2006) https://doi.org/10.1111/j.1600-0870.2006.00195.x

[21] Varotsos, C.A., Efstathiou, M.N., Cracknell, A.P.: On the scaling effect in global surface air temperature anomalies. Atmospheric Chemistry and Physics **13**, 5243–5253 (2013) https://doi.org/10.5194/acp-13-5243-2013

[22] Spanjers, R., Klein Tank, A., Selten, F., *et al.*: Increased persistence of warm and wet winter weather in recent decades in north-western europe. Communications Earth & Environment **6**, 52 (2025) https://doi.org/10.1038/s43247-025-01901-7

[23] Fraedrich, K., Larnder, C.: Scaling regimes of composite rainfall time series. Tellus A **45**(4), 289–298 (1993) https://doi.org/10.1034/j.1600-0870.1993.t01-3-00004.x

[24] Pelletier, J.D., Turcotte, D.L.: Long-range persistence in climatological and hydrological time series: analysis, modeling and application to drought hazard assessment. Journal of Hydrology **203**(1–4), 198–208 (1997) https://doi.org/10.1016/S0022-1694(97)00102-9

[25] Yang, L., Fu, Z.: Process-dependent persistence in precipitation records. Physica A **527**, 121459 (2019) https://doi.org/10.1016/j.physa.2019.121459

[26] Dong, B., Jiang, P., Liang, J., Wang, B.: Whether the cmip5 models can reproduce the long-range correlation of daily precipitation? Atmosphere **12**(10), 1334 (2021) https://doi.org/10.3390/atmos12101334

[27] Bunde, A., Büntgen, U., Ludescher, J., Luterbacher, J., Storch, H.: Is there memory in precipitation? Nature Climate Change **3**(3), 174–175 (2013) https://doi.org/10.1038/nclimate1830

[28] Takalo, J.J.: Persistence of temperature and precipitation: from local to global anomalies. Annals of Geophysics **64**(6), 654 (2021) https://doi.org/10.4401/ag-8618

[29] Lenton, T.M., Dakos, V., Bathiany, S., Scheffer, M.: Observed trends in the magnitude and persistence of monthly temperature variability. Scientific Reports **7**, 5940 (2017) https://doi.org/10.1038/s41598-017-06382-x

[30] Sippel, S., Zscheischler, J., Heimann, M., Otto, F.E.L., Peters, J., Mahecha, M.D.: Quantifying changes in climate variability and extremes: Pitfalls and their overcoming. Geophysical Research Letters **42**(22), 9990–9998 (2015) https://doi.org/10.1002/2015GL066307

[31] Hansen, J., Ruedy, R., Sato, M., Lo, K.: Global surface temperature change. Reviews of Geophysics **48**(4), 4004 (2010) https://doi.org/10.1029/2010RG000345

[32] Harris, I., Jones, P.D., Osborn, T.J., Lister, D.H.: Version 4 of the cru ts monthly high-resolution gridded multivariate climate dataset. Scientific Data **7**, 109 (2020) https://doi.org/10.1038/s41597-020-0453-3

[33] Peng, C.-K., Buldyrev, S.V., Havlin, S., Simons, M., Stanley, H.E., Goldberger, A.L.: Long-range correlations in nucleotide sequences. Nature **368**(6471), 546–549 (1994)

[34] Peng, C.-K., Havlin, S., Stanley, H.E.G., L, A.: Quantification of scaling exponents and crossover phenomena in nonstationary heartbeat time series. Chaos: An Interdisciplinary Journal of Nonlinear Science **5**(1), 82–87 (1995)